Electronic Structure Dependence on the Density, Size and Shape of Ge/Si Quantum Dots Array

Ming-Yi Lee*, Yi-Chia Tsai*, Yiming Li* and Seiji Samukawa†
*Institute of Communications Engineering, Department of Electrical and Computer Engineering
National Chiao Tung University, Hsinchu 300, Taiwan (e-mail: ymli@faculty.nctu.edu.tw (Y. Li))
†Institute of Fluid Science and WPI-AIMR, Tohoku University, Sendai 980-8577, Japan

INTRODUCTION

Among the next-generation ultra-high efficiency photovoltaics technologies, a promising candidate is the use of semiconductor quantum dots (QDs). The QDs work as the intermediate band in solar cell and dramatically increase the efficiency because of their ability to absorbing sub-bandgap photons through the two-photon transition [1]. When uniform QDs are closely packed as the superlattice, wavefunction of each QD couples with neighboring QDs to broaden the discrete quantum levels to form finite-width miniband, which is a key parameter to determine two-photon transition. Within the envelop-function framework, a 3D finite element method that surmounts theoretical approximations of the multi-dimensional Kronig-Penney method has recently been developed to simulate miniband structure and density of states (DoS) [2]. In this work, the electron structure dependence on the density, size and shape of Ge/Si QDs array is studied in further to instruct realistic QDs fabrication and design.

THE COMPUTATIONAL MODEL

For the periodic superlattice, the electronic structure is numerically solved by Eq. (1) under Bloch theorem as Fig. 1. First, a unit cell formed by the primitive vectors is defined. Then, based on the symmetry of superlattice, the $\boldsymbol{k}$-points space is defined in an IBZ. To get band structure $E_{n,k}$ and bloch function $u_k(\boldsymbol{r})$, Eq. (1) is discretized within a unit cell in real space and solved by a FEM solver for each sampling $\boldsymbol{k}$-point in IBZ. Finally, the DoS, a key parameter for electronic and optical applications of semiconductor system, is calculated numerically using an improved triangle method [3] by Eq. (2).

RESULTS AND DISCUSSION

Fig. 2 shows the calculated band dispersion relation for QD in dimension of the radius 3 nm and the thickness 4 nm [4] and the interdot space 2.3 nm. The energy distribution in IBZ for the lowest four bands is shown in Fig. 3. The energy for the ground band is distributed isotropically in $\boldsymbol{k}$-space and minimum in Γ-point. The energy for the first and second excited bands are constant in k_y and k_x direction respectively while the energy for the third excited band is distributed isotropically in $\boldsymbol{k}$-space. These distributions are closely related to their wavefunctions. Fig. 2b shows the isosurface of wave function within Ge QD at Γ-point ($\boldsymbol{k} = 0$) of IBZ for lowest four bounded-states. The ground state has ellipsoid surface without nodes as the expected s-orbit. The next three states show a two-fold degenerate p-orbit due to symmetry of x-y plane and non-degenerate p-orbit along z-direction. These energy distributions and wave functions reveal the symmetry of the QDs superlattice.

Fig. 4 presents the DoS for QDs superlattice with varied interdot space from 0.3 nm to 3.3 nm. As the interdot space decreasing, i.e. QDs density increasing, QDs interaction between discrete levels increases and miniband crossing phenomenon occurs especially for higher excited states. Because the highest excited states are mixed and become continuous energy levels to Si barrier, the effective bandgap of bulk Si decreases.

In Fig. 5, the energy level of the ground band becomes lower with varied thickness from 2 nm to 8 nm because of the weaker confinement in z-direction as expected. Meanwhile, the band width less depends on the thickness because the interaction between QDs is strongly related to the distance between QDs in x-y plane. The significant dependence of band structure on QDs symmetry is revealed for the third excited band $E_{3,k}$ of QDs with the thickness 4 nm, which is non-degenerate p-orbit along z-direction in Fig. 2b. In Fig. 6, this p-orbit along z-direction have much weaker confinement and becomes the first excited band for QDs thickness 8 nm. On the other hand, the energy level goes lower and band width goes smaller with the QDs radius in Fig. 7 because of the weaker confinement and larger distance between QDs in x-y plane.

Fig. 8 presents the calculated energy levels and bandwidth of ground band as functions of the QDs volume for three different QDs shapes with the same base radius (3 nm). Bigger the QDs volume, lower energy level and larger band width. The most sensitive to the dot volume is the disk-shape and the least is the cone-shape. This phenomenon is due to the stronger z-confinement and interaction in x-y plane for disk-shape QDs than that for the other shapes.

In summary, we have reported the miniband structure dependence on the density, size and shape of Ge/Si QDs array. The QDs density has strong impact on the QDs interaction and miniband width. Meanwhile, the QDs volume and shape affect the quantum confinement through the geometric symmetry.

REFERENCES

[1] A. Luque *et al.*, *Phys. Rev. Lett.*, vol. 78, p. 5014, 1997.
[2] M.-Y. Lee *et al.*, *IEEE Trans. Electron Devices*, submitted for publication.
[3] J.-H. Lee *et al.*, *Phys. Rev. B*, vol. 66, p. 233102, 2002.
[4] M. Igarashi *et al.*, *Appl. Phys. Lett.*, vol. 101, p. 063121, 2012.

ISBN 978-0-692-50554-0

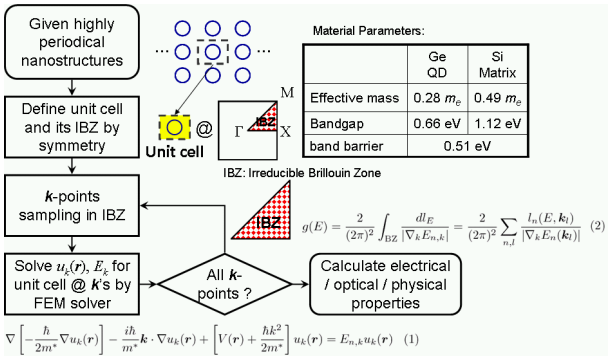

Fig. 1. The simulation flow chart for an in-plane 3D QDs square superlattice and material parameters used for simulation.

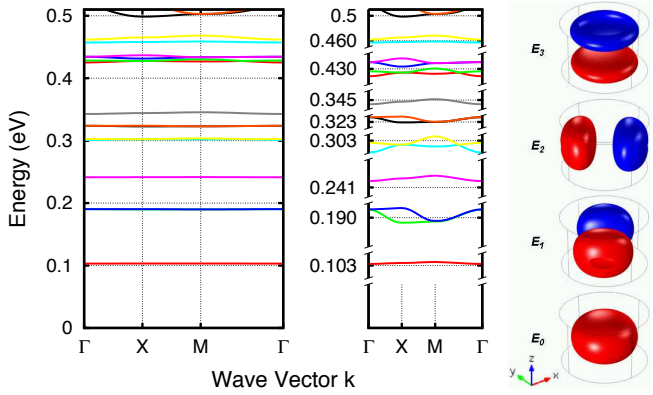

(a) (b)

Fig. 2. (a) The band dispersion relation for 3D in-plane Ge/Si QDs superlattice with QD's radius 3 nm, thickness 4 nm and interdot space 2.3 nm. The right figure breaks energy axis into several segments in different scale to highlight the profile of each quantum level. (b) The isosurface of wave function within QD at Γ-point of IBZ for lowest four bounded-states: s-orbit E_0, degenerate p-orbit E_1 and E_2, and non-degenerate p-orbit E_3.

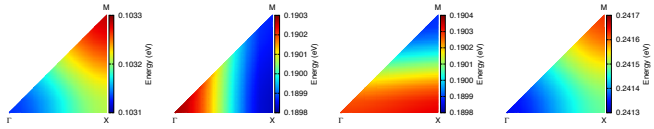

(a) (b) (c) (d)

Fig. 3. The energy distribution in IBZ for (a) ground bounded-band $E_{0,k}$, (b) first excited bounded-band $E_{1,k}$, (c) second excited bounded-band $E_{2,k}$, and (d) third excited bounded-band $E_{3,k}$.

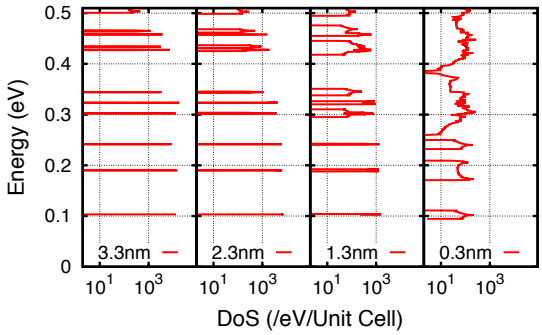

Fig. 4. The density of states for Ge/Si QDs square superlattice with QD radius 3 nm, thickness 4 nm, and varied interdot space from 3.3 nm to 0.3 nm.

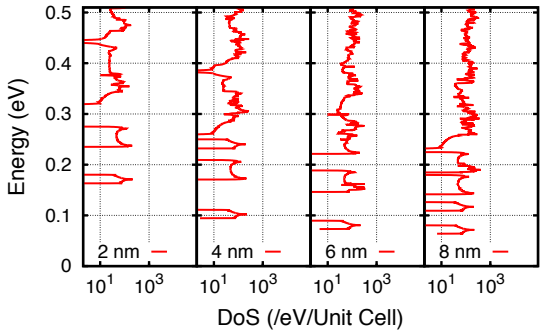

Fig. 5. The density of states for Ge/Si QDs square superlattice with QD radius 3 nm, interdot space 0.3 nm, and varied thickness from 2 nm to 8 nm.

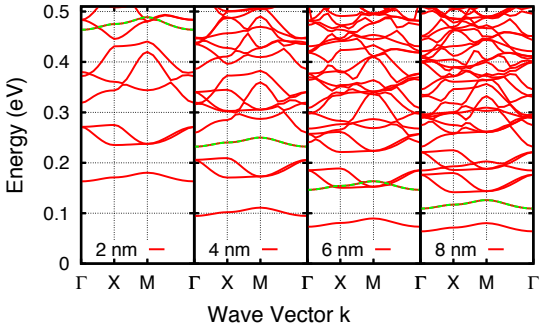

Fig. 6. The band structures for Ge/Si QDs square superlattice with QD radius 3 nm, interdot space 0.3 nm, and varied thickness from 2 nm to 8 nm. The highlight band with p-orbit symmetry in z-direction (green dash line) shows much more dependence on the QDs thickness.

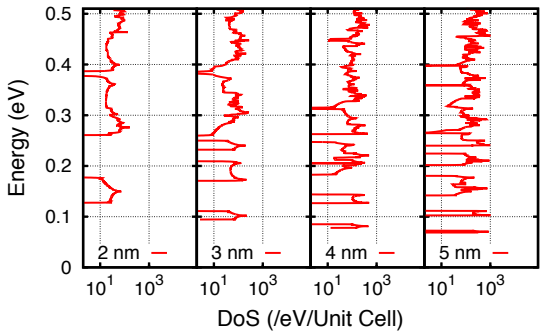

Fig. 7. The density of states for Ge/Si QDs square superlattice with QD thickness 4 nm, interdot space 0.3 nm and varied radius from 2 nm to 5 nm.

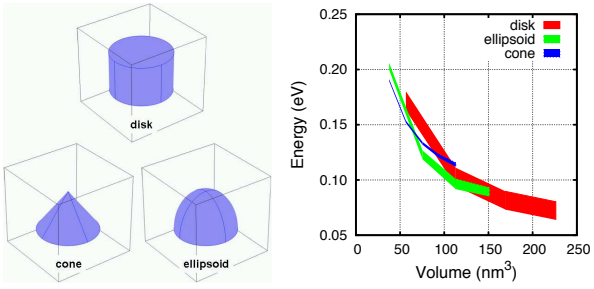

(a) (b)

Fig. 8. (a) Three kinds of QDs shape used for comparison. (b) The energy level of ground band versus QDs volume for Ge/Si QDs square superlattice with different QDs shape.